九州工業大学学術機関リポジトリ

Kyutacar

Kyushu Institute of Technology Academic Repository

Dependence of photocatalytic activity on aspect ratio of a brookite TiO2 nanorod and drastic improvement in visible light responsibility of a brookite TiO2 nanorod by site-selective modification of Fe3+ on exposed faces

	Ohno Teruhisa, Higo Takayoshi, Saito Hirofumi, Yuajn Saisai, Jin Zhengyuan, Yang Yin, Tsubota Toshiki
journal or publication title	Journal of Molecular Catalysis A: Chemical
volume	396
page range	261-267
year	2014-10-14
URL	http://hdl.handle.net/10228/00006881

Dependence of photocatalytic activity on aspect ratio of a brookite TiO_2 nanorod and drastic improvement in visible light responsibility of a brookite TiO_2 nanorod by site-selective modification of Fe^{3+} on exposed faces

Teruhisa Ohno[a,b,c,*], Takayoshi Higo[a], Hirofumi Saito[a], Saisai Yuajn, Zhengyuan Jin[a], Yin Yang[a], Toshiki Tsubota[a]

[a] Department of Materials Science, Faculty of Engineering, Kyushu Institute of Technology, 1-1 Sensuicho, Tobata, Kitakyushu 804-8550, Japan

[b] JST, PRESTO, 4-1-8 Honcho Kawaguchi, Saitama 332-0012, Japan

[c] JST, ACT-C, 4-1-8 Honcho Kawaguchi, Saitama 332-0012, Japan

AUTHOR EMAIL ADDRESS: murakami@che.kyutech.ac.jp

* CORRESPONDING AUTHOR: Teruhisa Ohno

TEL & FAX: +81-93-884-3318, EMAIL ADDRESS: tohno@che.kyutech.ac.jp

Abstract

Exposed crystal face-controlled brookite titanium(IV) oxide (TiO_2) nanorods with various aspect ratios were prepared by a hydrothermal process with or without PVA or PVP as an aspect reagent.   The nanorod-shaped brookite TiO_2 had larger {210} and smaller {212} exposed crystal faces, which were assigned by TEM with the SAED technique.   Their aspect ratios were greatly influenced by the addition of PVA or PVP as an aspect ratio control reagent to the reaction solution used in the hydrothermal

1

treatment. The photocatalytic activity for decomposition of acetaldehyde increased with increase in the aspect ratio because the surface area ratio of {210} to {212} exposed crystal faces, which are attributed to reduction and oxidation sites, respectively, became more optimal.

The {212} exposed crystal faces of surface-controlled brookite TiO_2 were site-selectively modified with trivalent iron(III) (Fe^{3+}) ions by utilizing the adsorption property of iron(III)/iron(II) (Fe^{3+}/Fe^{2+}) ions.   The brookite TiO_2 nanorod with site-selective modification of Fe^{3+} ions showed much higher photocatalytic activity than that of commercial brookite TiO_2 loaded with Fe ions under visible-light irradiation because of the separation of redox sites.   In other words, oxidation and reduction proceed over Fe^{3+} ion-modified {212} faces of the TiO_2 surface and on {210} faces of the TiO_2 surface without modification of Fe^{3+}, respectively.

Keywords

Photocatalyst; titanium(IV) oxide; brookite TiO_2 nanorod; separation of redox sites; visible light responsibility

Introduction

Much interest has recently been shown in environmental purification by utilizing the self-cleaning effect of a semiconductor photocatalyst [1,2].   Among the various kinds of semiconductor photocatalyst, titanium(IV) oxide (TiO_2) is the most

2

suitable photocatalyst for application to environmental purification from the viewpoint of chemical stability, availability and no toxic properties. Photocatalytic activity over semiconductor particles is thought to depend on the physical and chemical properties of the photocatalyst, such as its crystal structure, specific surface area, particle size, and defect density[3]. Therefore, optimizing these properties has been the conventional strategy for enhancing photocatalytic activity, though the most suitable property to optimize for a specific reaction differs depending on the reaction substrate.

Since the report on titanium(IV) oxide (TiO_2) with specific exposed crystal faces by Ohno et al. in 2002[4], various groups have reported TiO_2 with control of exposed crystal faces[5-19]. Our group has succeeded in synthesizing shape-controlled anatase rutile and brookite TiO_2 with photocatalytic properties depending on specific exposed crystal faces due to control of reaction sites[20-23]. The results imply that the exposed crystal face of a TiO_2 photocatalyst is an important factor for improvement of its photocatalytic activity. This is reasonable since the surface energy, chemical surface state, and number and energy state of defective sites predominantly depend on the atomic arrangement of exposed crystal faces[24-26].

Decahedral TiO_2 having an anatase phase with {101} and {001} exposed crystal faces[4,5,8,10-14,23], shape-controlled TiO_2 having a brookite phase[27-32], and dodecahedral rutile TiO_2 with {110} and {101} or {110} and {111} exposed crystal faces[6,7,20] have been synthesized as well-defined TiO_2 particles. Formation of these exposed crystal faces requires the use of inorganic or organic compounds as

3

shape-control reagents[6-8,11,20,23] specific precursors[9,13,14] and specific preparation conditions.[12][29-32]

Ohno et al. reported that the photocatalytic activity of shape-controlled TiO_2 nanorods having a rutile phase depended on their exposed crystal faces, which could be controlled by using shape-control reagents or chemical etching.[21] The exposed crystal faces of shape-controlled rutile TiO_2 nanorods were assigned to {110} and {111} crystal faces, which were respectively attributed to reduction and oxidation sites.[20] In addition, shape-controlled rutile TiO_2 rods with various aspect ratios were successfully prepared by a two-step synthesis involving hydrolysis and hydrothermal processes, and their photocatalytic activities were shown to strongly depend on the aspect ratio.[33]

In the present study, we prepared shape-controlled brookite TiO_2 nanorods with various aspect ratios by a hydrothermal process in the presence of a shape-control agent (polyvinyl alcohol (PVA) and/or polyvinyl pyrrolidone (PVP)). The exposed crystal faces of brookite TiO_2 nanorods were successfully assigned to crystal faces that are different from those of rutile TiO_2 nanorods. Reactivity on the exposed crystal faces was also evaluated. The exposed crystal faces of brookite TiO_2 nanorods were analyzed as a function of the aspect ratio of shape-controlled brookite TiO_2 nanorods, and the dependence of photocatalytic activity for acetaldehyde decomposition on the aspect ratio was examined. In addition, shape-controlled brookite TiO_2 nanorods with specific exposed crystal faces, which had quite high visible light activity, were modified with iron(III) (Fe^{3+}) ions. In our previous study, modification of rutile TiO_2 with Fe^{3+}

ions greatly improved photocatalytic reaction under visible-light irradiation because the Fe^{3+} ions worked as sensitizers for visible light. Moreover, characteristic adsorption properties of Fe^{3+}/Fe^{2+} ions on TiO_2, which are strongly dependent on valence states of iron ions, induced site-selective adsorption on specific exposed crystal faces of brookite TiO_2 nanorods.

2. Experimental

2.1. Materials

A titanium precursor (titanium ethoxide) was purchased from Sigma-Aldrich. Hydrogen peroxide (30%), ammonia (25%), glycolic acid, polyvinyl alcohol (PVA), and polyvinyl pyrolidone (PVP) were purchased from Wako Pure Chemical Industries, Ltd. Titanium(IV) bis(ammonium lactate) dihydroxide (TALH) and urea were purchased from Sigma-Aldrich. Glycolic acid was used to control the crystallinity and morphology of brookite TiO_2 particles. Commercial brookite TiO_2 powder was obtained from Kojundo Chemical Laboratory Co., Ltd. Other chemical reagents used in the present study were commercial products without further treatments.

2.2. Procedure for preparation of brookite TiO_2 nanorods without a polymer

Morphology-controlled brookite TiO_2 nanorods with {210} and {212} exposed crystal faces were prepared by hydrothermal synthesis [34, 35-37].

The typical procedure for preparation of shape-controlled brookite TiO$_2$ nanorods is as follows. Amorphous titanium hydroxide particles (12.5 mmol) were dispersed in 30% hydrogen peroxide (40 cm^3). Then 25% ammonia (10 cm^3) and glycolic acid (18.75 mol) were added. After stirring the solution at ca. 60 °C for 6 h to remove the excess amount of hydrogen peroxide and ammonia, an orange gelled compound was obtained. The gelled compound was dispersed in deionized water and pH of the solution was adjusted to 10 by addition of ammonia. Then the volume of the solution was adjusted (50.0 cm^3) by addition of deionized water, and the solution in a Teflon bottle sealed with a stainless jacket was heated at 200 °C for 48 h in an oven. After hydrothermal treatment, the residue was washed with deionized water until ionic conductivity of the supernatant was <10 μS cm^{-1}. The particles were dried under reduced pressure at 60 °C for 12 h.

2.3. Procedure for preparation of brookite TiO$_2$ nanorods with a polymer as an aspect control reagent

Amorphous titanium hydroxide particles (12.5 mmol) were dispersed in 30% hydrogen peroxide (40 cm^3). Then 25% ammonia (10 cm^3) and glycolic acid (18.75 mmol) were added, and yellow peroxo titanic acid (PTA) solution was obtained. An aqueous solution containing an appropriate amount of PVA or PVP (5, 25, 50 mg) was added to the PTA solution. After stirring the solution at room temperature for 6 h to remove the excess amount of hydrogen peroxide and ammonia, an orange gelled compound was obtained. The gelled compound was dispersed in deionized water and

pH of the solution was adjusted to 10 by addition of ammonia. Then the volume of the solution was adjusted (50.0 cm^3) by addition of deionized water, and the solution in a Teflon bottle sealed with a stainless jacket was heated at 200 ^{o}C for 48 h in an oven. After hydrothermal treatment, the residue in the Teflon bottle was washed with milli-Q water until ionic conductivity of the supernatant was < 10 μS cm^{-1}. The particles were dried under reduced pressure at 60 ^{o}C for 12 h.

2.4. Procedure for preparation of brookite TiO$_2$ nanorods using titanium bis(ammonium lactate) dihydroxide (TALH) as a starting material[30]

Five milliliters of TALH aqueous precursor (50%) and an aqueous solution containing urea (7M) were mixed and then deionized water was added to reach a final volume of 50 cm^3. The resulting solution was transferred into a Teflon cup. The Teflon bottle sealed with a stainless jacket was heated at 230 ^{o}C for 48 h in an oven. The resulting powder was separated by centrifugation and washed with milli-Q water until ionic conductivity of the supernatant was < 10 μS cm^{-1}. The particles were dried under reduced pressure at 60 ^{o}C for 12 h.

2.5. Non-site-selective modification of the entire surface with Fe^{3+} ions

An aqueous suspension containing shape-controlled brookite TiO$_2$ nanorods and an aqueous solution of iron(III) nitrate (Fe(NO$_3$)$_3$) was stirred for 6 h under an aerated condition. After stirring, the supernatant and residue were separated by filtration, and the residue was washed with deionized water several times until the ionic

7

conductivity of the supernatant was < 10 µS cm^{-1} in order to remove NO_3^- ions. The particles were then dried under reduced pressure.

2.6. Site-selective modification of specific exposed faces with Fe^{3+} ions

An aqueous suspension containing each brookite TiO_2 and an aqueous solution of $Fe(NO_3)_3$ with ethanol (30 cm^2) was stirred for 6 h under an aerated condition. The stirring was carried out under UV irradiation with a 500-W super-high-pressure mercury lamp (Ushio, SX-UI501UO), the light intensity of which was 1.0 mW cm^{-2}. The supernatant and residue were separated by filtration immediately after the 6 h of stirring. The residue was washed with deionized water several times until the ionic conductivity of the supernatant was <10 µS cm^{-1}, and then the particles were dried under reduced pressure.

2.7. Characterization

The crystal structures of the powders were confirmed by using an X-ray diffractometer (Rigaku, MiniFlex II) with Cu Kα radiation ($\lambda = 1.5405$ Å). Diffuse reflectance (DR) spectra were measured using a UV-VIS spectrophotometer (Shimadzu, UV-2500PC) equipped with an integrating sphere unit (Shimadzu, ISR-240A). The specific surface areas of the particles were determined with a surface area analyzer (Quantachrome, Nova 4200e) by using the Brunauer-Emmett-Teller equation. The morphology of prepared TiO_2 particles was observed by using transmission electron microscopy (TEM; Hitachi, H-9000NAR) and scanning electron microscopy (SEM;

JEOL, JSM-6701FONO). The net amount of Fe^{3+} ions on the TiO_2 surface was estimated by analysis of the filtrate with inductively coupled plasma optical emission spectroscopy (ICP-OES; Shimadzu, ICPS-8000). X-ray photoelectron spectra (XPS) of the TiO_2 particles were measured using a photoelectron spectrometer (JEOL, JPS90SX) with an Mg Kα source (1253.6 eV). The shift of binding energy was corrected using the C 1s level at 284.6 eV as an internal standard.

2.8. Photocatalytic decomposition of toluene over pure brookite TiO_2 nanorods under UV light and photocatalytic decomposition of acetaldehyde over brookite TiO_2 nanorods with site-selective Fe^{3+} modification

Photocatalytic activities of samples were evaluated by photocatalytic decomposition of toluene. One hundred milligrams of powder, which had complete extinction of incident radiation, was spread on a glass dish, and the glass dish was placed in a 125 cm^3 Tedlar bag (AS ONE Co. Ltd.). Five hundred parts per million of gaseous acetaldehyde or one hundred parts per million of gaseous toluene was injected into the Tedlar bag, and photoirradiation was performed at room temperature after the toluene had reached adsorption equilibrium. The gaseous composition in the Tedlar bag was 79% of N_2, 21% of O_2, < 0.1 ppm of CO_2 and 100 ppm or 500 ppm of toluene, and relative humidity was ca. 30%. A light-emitting diode (Nichia, NCCU033), which emitted light at a wavelength of ca. 365 nm and an intensity of 0.1 mW cm^{-2}, was used as the light source for photocatalytic evaluation under UV light. A light-emitting diode (LED; Lumileds, Luxeon LXHL-NRR8),

which emitted light at a wavelength of ca. 455 nm with an intensity of 1.0 mW cm^{-2}, was also used for visible light irradiation.   The emission spectrum of the LED is shown in Fig. 1.   The concentrations of acetaldehyde and carbon dioxide (CO_2) were estimated by gas chromatography (Shimadzu, GC-8A, FID detector) with a PEG-20 M 20% Celite 545 packed glass column and by gas chromatography (Shimadzu, GC-9A, FID detector) with a TCP 20% Uniport R packed column and a methanizer (GL Sciences, MT-221), respectively.
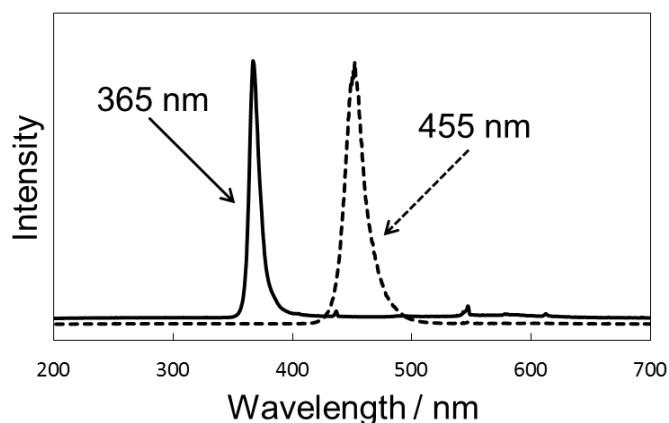
Fig. 1   Emission spectrum of the LED (365 or 455 nm)

3. Results and discussion

3.1. Morphology analysis of prepared brookite TiO$_2$ nanorods

Fig. 2 shows XRD patterns of the prepared brookite TiO_2 with and without PVA or PVP (50 mg) and also brookite TiO_2 using TALH as a starting material.   All prepared samples were attributed to a single-phase brookite TiO_2 structure.
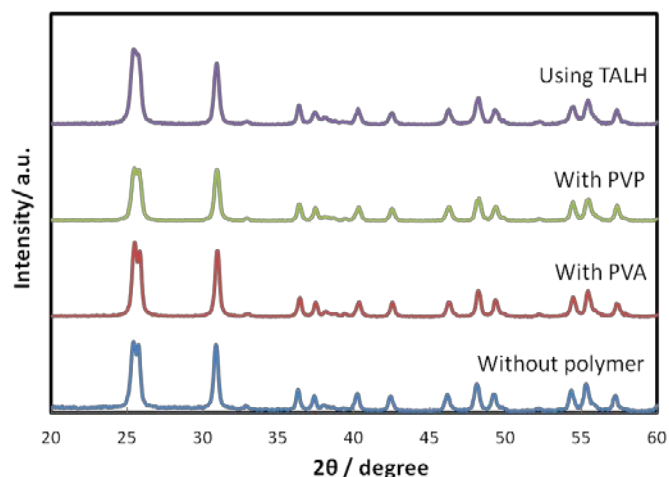
10

Fig. 2　XRD pattern of the prepared brookite TiO$_2$

Fig. 3 shows a TEM image of brookite TiO$_2$ without a polymer. rod-like morphology of

brookite TiO$_2$ with a length of 100 nm, width of 25 nm and an aspect ratio of 2.7 was

observed.　Relative surface area of the prepared brookite TiO$_2$ nanorod was 47 m^2 g^{-1}.

Assignment of exposed crystal faces was confirmed by TEM and selected area electron

diffraction (SAED) analysis (Fig. 4).　The prepared brookite TiO$_2$ showed a nanorod

shape with large {212} and small {210} exposed crystal faces.

　TEM and SEM images of aspect ratio controlled brookite TiO$_2$ by addition of the

PVA or PVP polymer (Fig . 5).

　　　The aspect ratio of brookite TiO$_2$ nanorods was decreased by addition of PVA

or PVP.　The effect of addition of PVA for aspect ratio control of brookite TiO$_2$

nanorods was greater than that of PVP as shown in Fig. 5.　These results indicate that

addition of 50 mg of PVA was sufficient to prepare brookite TiO$_2$ particles with the

smallest aspect ratio (Fig. 5). The aspect ratio (AR) and TEM images of the prepared
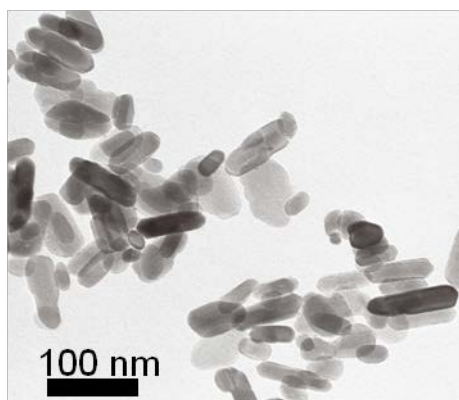
samples were summarized in Fig. 6.

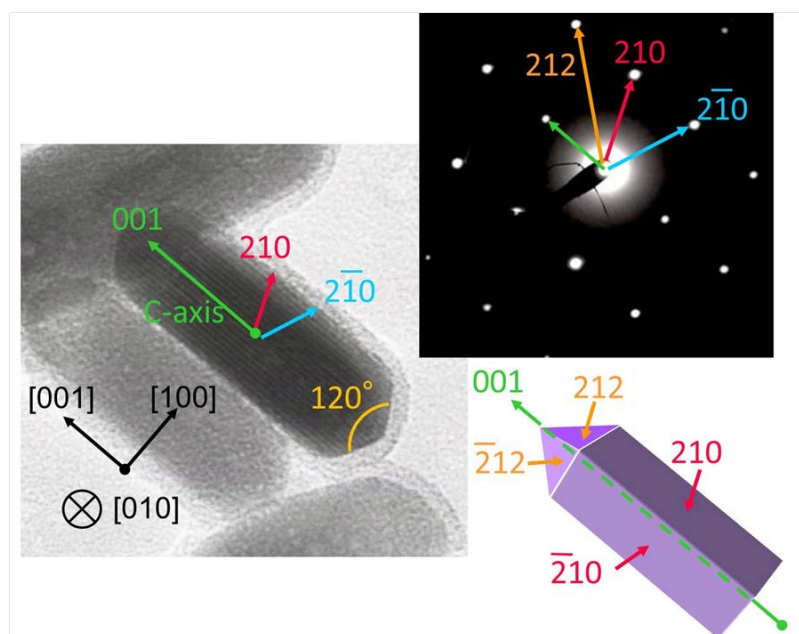Fig. 3   TEM image of the prepared brookite TiO$_2$ without a polymer

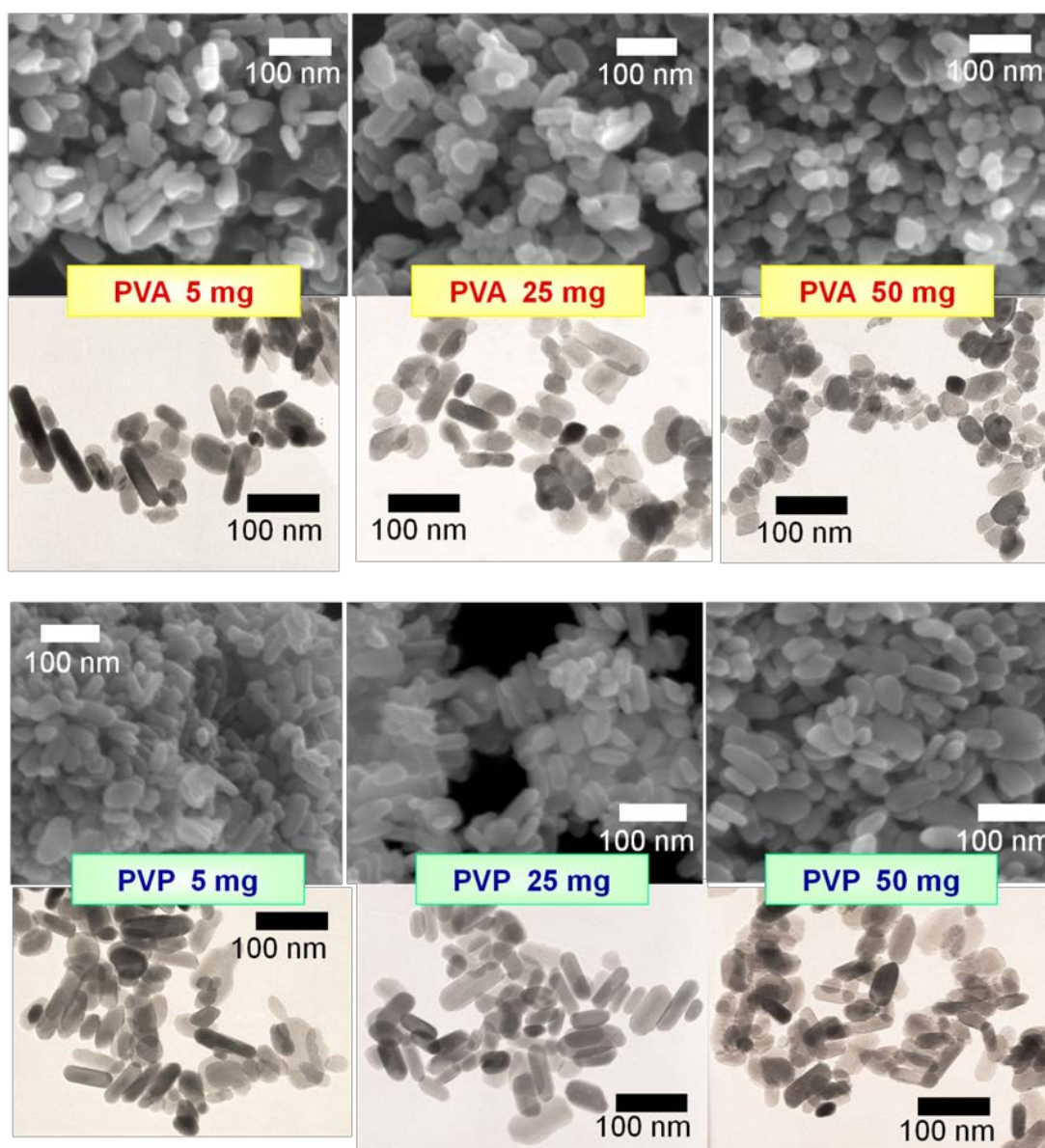Fig. 4   SAED analysis of the prepared brookite TiO$_2$ without a polymer

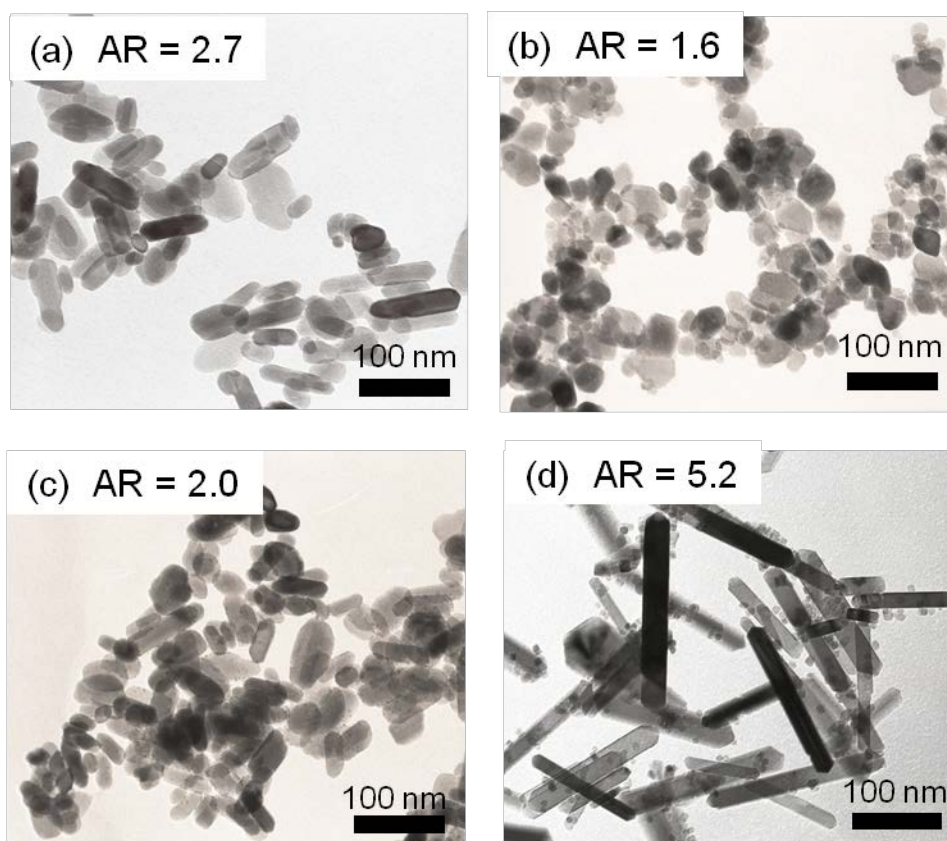Fig. 5   The influence in aspect ratio of brookite TiO$_2$ nanorods by addition of PVA or PVP

Fig. 6   TEM image of the prepared brookite TiO_2 :

(a) without a polymer (b)With PVA (50 mg)

(c) With PVP (50 mg) (d) Using TALH

3.2. Correlation between aspect ratio of brookite TiO_2 nanorods and photocatalytic activity for toluene degradation under UV light

The photocatalytic activities of the prepared samples for decomposition of toluene were evaluated.   Fig. 7 shows CO_2 evolution as a result of toluene decomposition over several kinds of prepared TiO_2 nanorods under UV irradiation for 8 h by using LED at a wavelength of 365 nm as a right source. The amount of CO_2 evolved varied greatly

14

among the samples.   The aspect ratio of a brookite TiO_2 nanorod with specific exposed crystal faces is rather sensitive to photocatalytic activity for toluene decomposition. Photocatalytic activity for toluene decomposition on a photoirradiated brookite TiO_2 nanorod with a larger aspect ratio was higher than that on a nanorod with a smaller aspect ratio.   This result suggested that photocatalytic toluene decomposition was drastically improved by controlling the ratio of exposed reduction sites to oxidation sites on the surface of the brookite TiO_2 nanorod.   Under optimized conditions, reduction sites on the surface of the brookite TiO_2 nanorod should be predominantly exposed as shown in Fig. 7.   These results indicated that reduction of oxygen on the surfaces of the reduction sites of a brookite TiO_2 nanorod might be the rate-determining step for toluene oxidation over a brookite TiO_2 nanorod under UV light.
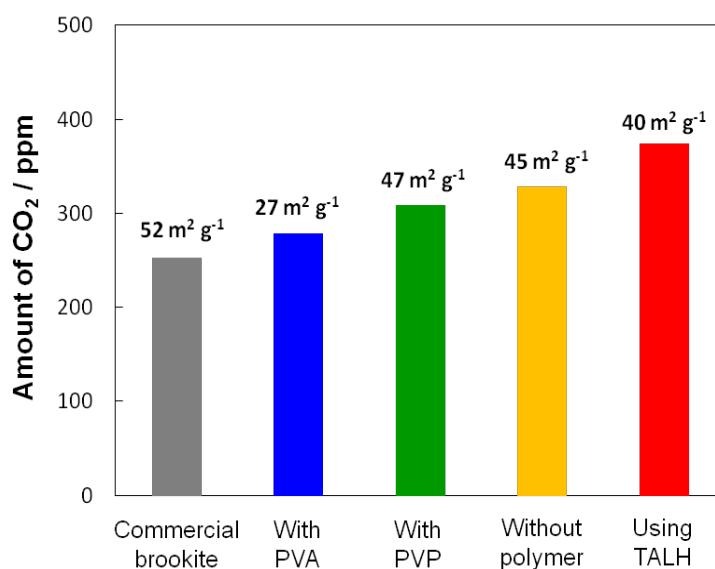

Fig. 7 CO_2 evolution as a result of toluene decomposition

over several kinds of prepared brookite TiO_2 under UV irradiation

for 8 h by using an LED at a wavelength of 365 nm

15

## 3.3. Properties of bare and Fe^{3+}-modified brookite TiO_2 nanorods

Among the several kinds of brookite TiO_2 including commercial brookite TiO_2, we selected brookite TiO_2 with PVP, brookite TiO_2 without a polymer, and commercial brookite TiO_2. We would like to discuss the relationship between visible light responsive photocatalytic activity and adsorption in visible region. Therefore, the absorption spectra of Fe^{3+} modified commercial TiO_2, with PVP, and without polymer, were analyzed. These samples showed the highest, second, lowest photocatalytic activities. Table 1 shows a summary of Fe^{3+}-modified brookite TiO_2 by two Fe^{3+} modification methods and the net amount of Fe^{3+} loaded on the prepared samples.

Table 1　A summary of Fe^{3+} modified prepared brookite TiO_2

Brookite TiO_2	Sample name	Loading amount / wt%	Loading method	Net amount / wt%
Commercial	Com-imp	0.05	Impregnation	0.043
Commercial	Com-photo	0.05	Hg lamp	0.033
With PVP	PVP-imp	0.05	Impregnation	0.041
With PVP	PVP-photo	0.05	Hg lamp	0.041
Without a polymer	No polymer-imp	0.05	Impregnation	0.042
Without a polymer	No polymer-photo	0.05	Hg lamp	0.035

The valence state of iron ions on TiO_2 particles was confirmed to be a trivalent state by XPS analyses.　UV light irradiation during Fe^{3+} modification decreased the net amount of Fe^{3+} ions on the TiO_2 surface, while almost the entire surface was modified with Fe^{3+} ions in the dark, in agreement with modification of a rutile TiO_2 nanorod with iron ions under UV light irradiation[38].　It has been reported that Fe^{2+} ions hardly adsorb on the TiO_2 surface compared to Fe^{3+} ions [39].　Therefore, it is thought that Fe^{2+} ions were

produced as a result of reduction of Fe^{3+} ions by photoexcited electrons in TiO_2 and then the Fe^{2+} ions desorbed from the TiO_2 surface. Reduction of Fe^{3+} ions efficiently proceeded on the surfaces of reduction sites of a brookite TiO_2 nanorod using ethanol as an hole scavenger. The reduction of Fe^{3+} ions was induced by efficient hole consumption resulting in electron accumulation in the TiO_2 nanorod. Reactivity assignment of exposed {210} and {212} crystal faces of a brookite TiO_2 nanorod were assigned to reduction and oxidation sites by photodeposition of PbO_2 and Pt nanoparticles, respectively, according to the previously reported technique[20-22]. These results indicated that reduction and oxidation on the brookite TiO_2 nanorod proceed predominantly on {210} and {212} exposed crystal faces, respectively (not shown here). Therefore, Fe^{3+} ions are expected to mainly adsorb on {212} faces under UV irradiation because Fe^{3+} ions on {210} faces desorb due to reduction of Fe^{3+} to Fe^{2+} (Scheme 1). The Fe^{2+} ions were recovered to Fe^{3+} ions as a result of reoxidation by oxygen and/or positive holes on {212} faces.
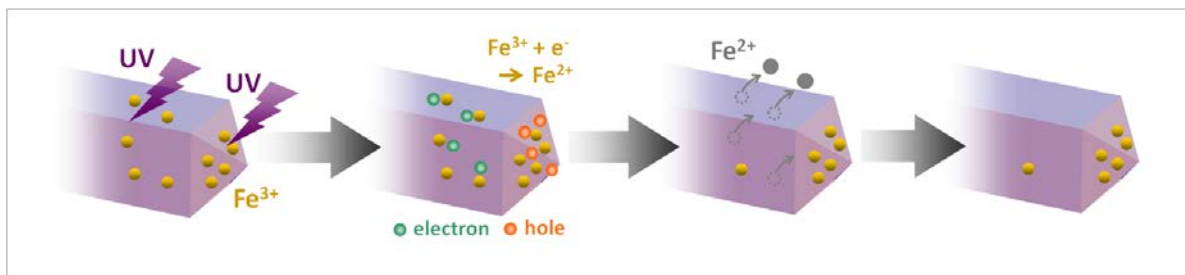
Scheme 1 Fe^{3+} ions are expected to mainly adsorb on {212} faces

under UV irradiation

Modification with Fe^{3+} ions induced a color change from white to pale yellow. Fig. 8 shows UV-VIS spectra of bare and Fe^{3+}-modified TiO_2. In the wavelength region between 400 and 500 nm of DR spectra, an increase in photoabsorption was observed. Photoabsorption was increased with an increase in the net amount of Fe^{3+} ions in the brookite TiO_2 nanorod.
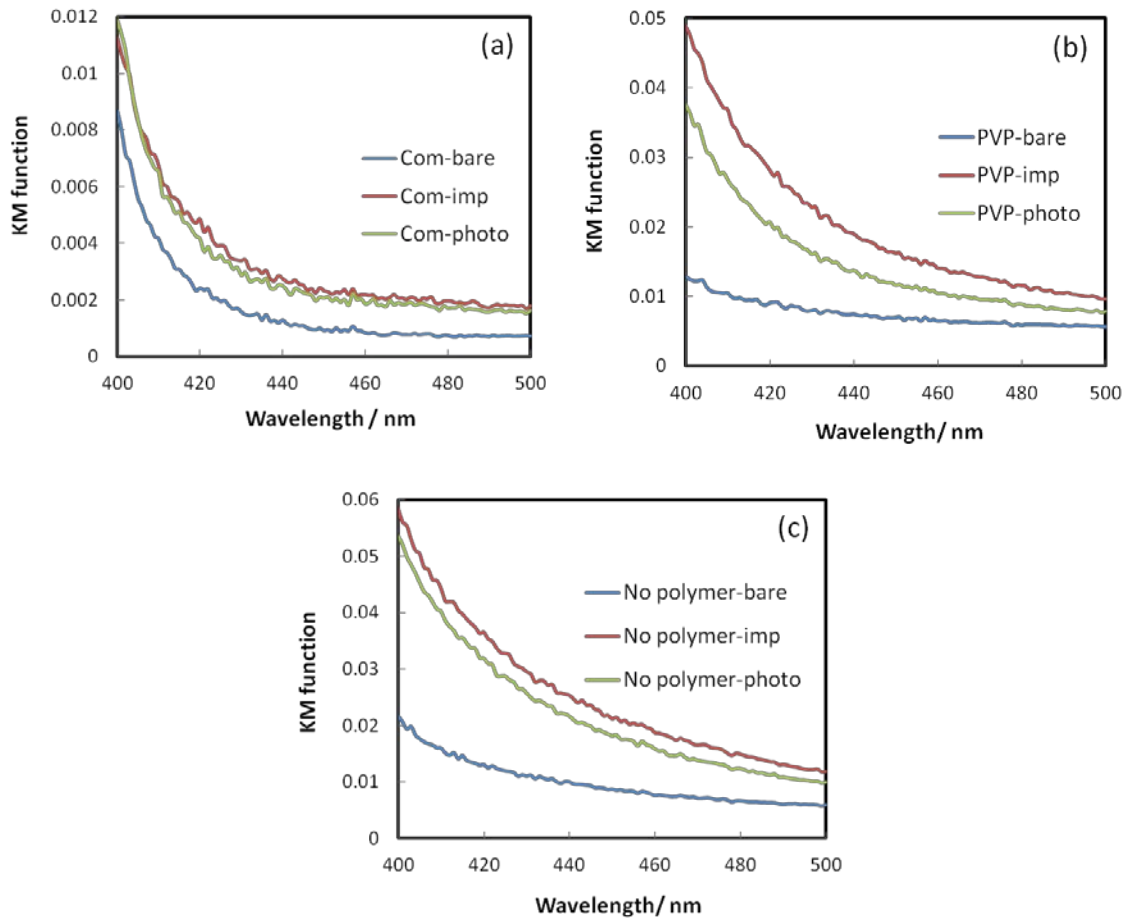
Fig. 8　UV-vis spectra of bare and Fe^{3+} (0.05 wt%)-modified brookite TiO_2 :

(a) commercial, (b) with PVP (50 mg), (c) without a polymer

3.4. Photocatalytic activity for decomposition of acetaldehyde under visible light irradiation

Fig. 9 shows dependence of the net amount of Fe^{3+} ions of the site-selective modified brookite TiO_2 on photocatalytic activity (CO_2 evolution after 24 h of photoirradiation).　Photocatalytic activity of the Fe^{3+}-modified brookite TiO_2

19

nanorod was much higher than that of Fe^{3+}-modified commercial brookite TiO_2 nanoparticles.   Under the same conditions, no photocatalytic activities of the brookite TiO_2 nanorod and commercial brookite TiO_2 nanoparticles without Fe^{3+} modification were observed for oxidation of acetaldehyde.   Moreover, photocatalytic activity of the Fe^{3+}-modified brookite TiO_2 nanorod showed dependence on the amount of Fe^{3+}. This indicates that Fe^{3+} ions on the brookite TiO_2 nanorod induced photocatalytic reaction under visible-light irradiation as follows [40]: (1) photoexcited Fe^{3+} ions injected electrons into TiO_2 and became an oxidized state of Fe^{3+} (Fe^{4+}), (2) injected electrons migrated in the bulk and reduced oxygen species on the TiO_2 surface and (3) the oxidized state of Fe^{3+} ions (Fe^{4+}) oxidized acetaldehyde and went back to the initial state of metal ions (Fe^{3+}). The amount of evolved CO_2 over nitrogen-doped TiO_2 (N-TiO_2; Sumitomo Chemical Co.) was about 180 ppm under the same experimental condition. Fe^{3+}-modified brookite TiO_2 nanorod showed higher photocatalytic activity than that of N-TiO_2, which is well known as conventional visible-light-responsive TiO_2.

Photocatalytic activity was increased by a small amount of Fe^{3+} modification because of the increase in visible light photoabsorption.   On the other hand, an excess amount of Fe^{3+} modification decreased photocatalytic activity presumably due to a decrease of reduction sites by coverage of the TiO_2 surface and/or formation of inactive aggregated Fe^{3+} species.   Therefore, increase in photocatalytic activity of the site-selective Fe^{3+}-modified brookite TiO_2 nanorod prepared by UV irradiation might be attributable to removal of an excess amount of Fe^{3+} for covering reduction sites or aggregation because UV irradiation decreased the net amount of Fe^{3+} ions.   In addition,

20

a site-selective Fe^{3+} modified brookite TiO_2 nanorod with a larger aspect ratio showed higher photocatalytic activity for acetaldehyde degradation than that of a brookite TiO_2 nanorod site-selectively modified with Fe^{3+} cations having a smaller aspect ratio. These results suggested that the rate-determining step of acetaldehyde oxidation under visible light might be oxygen reduction. Therefore, a site-selective Fe^{3+} modified brookite TiO_2 nanorod with a larger aspect ratio showed the highest activity for acetaldehyde oxidation under visible light.

The same modification method was applied to commercial brookite TiO_2, which has a spherical shape without specific exposed crystal faces. Fig. 9 shows the amount of CO_2 evolution as a result of decomposition of acetaldehyde over site-selective Fe^{3+}-modified commercial brookite TiO_2 nanoparticles under visible-light irradiation. Under that condition, it is thought that UV irradiation during Fe^{3+} modification does not induce site-selective modification on the particles because redox reaction proceeds in the neighboring sites without being separated. Therefore, a drastic decrease in photocatalytic activity was observed in the case of an excess amount of Fe^{3+} modification because the saturation limit of Fe^{3+} modification on the surface of commercial brookite TiO_2 nanoparticles was easily reached, resulting in a decrease in active sites by coverage of the brookite TiO_2 surface and/or formation of inactive aggregated Fe^{3+} species.
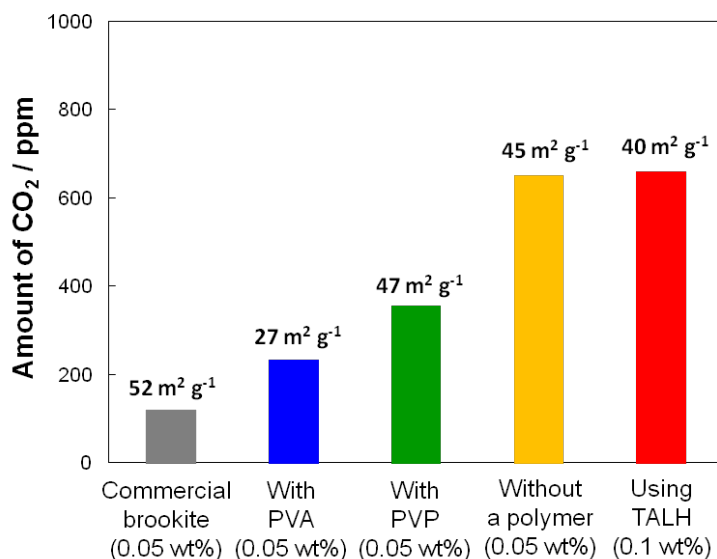
Fig. 9 CO_2 evolution as a result of acetaldehyde decomposition

over several kinds of Fe^{3+} -modified brookite TiO_2 under visible light

irradiation for 24 h by using an LED at a wavelength of 455 nm

4. Conclusions

Morphology-controlled brookite TiO_2 nanorods with a wide range of aspect

ratios (*AR* ~ 1.6-5.2) were successfully prepared.   The exposed crystal surfaces of

brookite TiO_2 nanorods were assigned to {210} and {212}.   Oxidation reaction

predominantly proceeded on the {212} facet, while the {210} facet was assigned to a

reduction site, resulting in the achievement of a charge separation and an improvement

of photocatalytic activity.   PVP and PVA were effective reagents for controlling the

aspect ratio of brookite TiO_2.   Dependence of photocatalytic activity for toluene

22

oxidation on aspect ratio of the morphology-controlled brookite TiO_2 nanorod was observed.

An improvement in the photocatalytic activity of a morphology- controlled brookite TiO_2 nanorod for acetaldehyde oxidation was achieved by site-selective modification of the exposed crystal surface of a brookite TiO_2 nanorod with Fe^{3+} ions.

Acknowledgements

FIGURE CAPTIONS

Figure 1.   Emission spectrum of the LED (365 or 455 nm)

Figure 2.   XRD pattern of the prepared brookite TiO_2

Figure 3.   TEM images of the prepared TiO_2 without a polymer

Figure 4.   SAED analysis of the prepared brookite TiO_2 without a polymer

Figure 5.   The influence in aspect ratio of brookite TiO_2 nanorods by addition of PVA or PVP (5, 25, 50 mg)

Figure 6.   TEM image of the prepared brookite TiO_2 :

(a) without a polymer, (b) with PVA (50 mg), (c) with PVP (50 mg), and (d) using TALH

Figure 7. CO_2 evolution as a result of toluene decomposition over several kinds of prepared brookite TiO_2 under UV irradiation for 8 h by using an LED at a wavelength of 365 nm

Figure 8.   UV-VIS spectra of bare and Fe^{3+} (0.05 wt%) -modified brookite TiO_2 : (a) commercial, (b) with PVP (50 mg), (c) without a polymer

Figure 9. CO_2 evolution as a result of acetaldehyde decomposition over several kinds of Fe3+-modified brookite TiO_2 under visible light irradiation for 24 h by using an LED at a wavelength of 455 nm

Scheme 1 Fe^{3+} ions are expected to mainly adsorb on {212} faces under UV irradiation

REFERENCES

(1) A. Fujishima, T. N. Rao, D. A. Tryk, J. Photochem. Photobiol. C: Photochem. Rev. 1 (2000) 1.

(2) M. R. Hoffmann, S. T. Martin, W. Choi, D. W. Bahnemann, Chem. Rev. 95 (1995) 69.

(3) O.O.P. Mahaney, N. Murakami, R. Abe, B. Ohtani, Chem. Lett. 38 (2009) 238.

(4) T. Ohno, K. Sarukawa, M. Matsumura, New. J. Chem. 26 (2002) 1167.

(5) K. Yoshinaga, M. Yamauchi, D. Maruyama, E. Mouri, T. Koyanagi, Chem. Lett. 34 (2005) 1094.

(6) E. Hosono, S. Fujihara, K. Kakiuchi, K. Imai, J. Am. Chem. Soc. 126 (2004) 7790.

(7) K. Kakiuchi, E. Hosono, H. Imai, T. Kimura, S. Fujihara, J. Cryst. Growth. 293 (2006) 541.

(8) D. Wang, J. Liu, Q. Huo, Z. Nie, W. Lu, R. E. Williford, Y. Jiang, J. Am. Chem. Soc. 2006, 128, 13670.

(9) F. Amano, T. Yasumoto, O.O.P. Mahaney, S. Uchida, T. Shibayama, B. Ohtani, Chem. Comm. (2009) 2311.

(10) D. Zhang, G. Li, H. Wang, K. M. Chan, J. C. Yu, Crystal Growth & Design 10 (2010) 1130.

(11) Y. Dai, C. M. Cobley, J. Zeng, Y. Sun, Y. Xia, Nano. Lett. 9 (2009) 6.

(12) F. Amano, O. O. P. Mahaney, Y. Terada, T. Yasumoto, T. Shibayama, B. Ohtani, Chem. Mater. 21 (2009) 2601.

(13) J. Li, D. Xu, Chem. Commun. 46 (2010) 2301.

(14) J. Li, Y. Yu, Q. Chen, J. Li, D. Xu, Cryst. Growth. Des. 10 (2010) 2111.

(15) Y. Li, N. Lee, D. Hwang, J. S. Song, E. G. Lee, S. Kim, Langmuir. 20 (2004) 10838.

(16) H. G. Yang, C. H. Sun, S. Z. Qiao, J. Zou, G. Liu, S. C. Smith, H. M. Cheng. G. Q. Lu, Nature. 453 (2008) 638.

(17) H. G. Yang, G. Liu, S. Z. Qiao, C. H. Sun, Y. G. Jin, S. C. Smith, J. Zou, H. M. Cheng, G. Q. Lu, J. Am. Chem. Soc. 131 (2009) 4078.

(18) J. Zhu, S. Wang, Z. Bian, S. Xie, C. Cai, J. Wang, H. Yang, H. Li, CrystEngComm 12 (2010) 2219.

(19) F. Amano, T. Yasumoto, O. O. P. Mahaney, S. Uchida, T. Shibayama, Top. Catal. 53 (2010) 455.

(20) E. Bae, N. Murakami, T. Ohno, J. Molec. Catal. A: Chem. 300 (2009) 72.

(21) E. Bae, T. Ohno, Appl. Catal. B: Environ. 91 (2009) 634-639.

(22) E. Bae, N. Murakami, M. Nakamura, T. Ohno, Appl. Catal. A: Gen. 380 (2010) 48.

(23) N. Murakami, Y. Kurihara, T. Tsubota, T. Ohno, J. Phys. Chem. C. 113 (2009) 3062-3069..

(24) P. M. Oliver, G. W. Watson, E. T. Kelsey, S. C. Parker, J. Mater. Chem. 7 (1997) 563.

(25) A.S. Barnard, P. Zapol, J. Phys. Chem. B. 108 (2004) 18435.

(26) A. S. Barnard, L. A. Curtiss, Nano Lett. 5 (2005) 1261.

(27) N. Murakami, T. Kamai, T. Tsubota, T. Ohno, Catal. Commun. 10 (2009) 963-966.

(28) N. Murakami, T. Kamai, T. Tsubota, T. Ohno, Cryst. Eng. Commun. 12 (2010) 532-537.

(29) M. Kobayashi, K. Tomita, V. Petrykin, S. Yin, T. Sato, M. Yoshimura, M. Kakihana, Solid. State. Phenomena. 124-126, 723-726 (2007)

(30) T. A. Kandiel, A. Feldhoff, L. Robben, R. Dillert, D. W. Bahnemann, Chem. Mater. 22 (2010) 2050-2060.

(31) H. Zhang, J. F. Banfield, J. Phys. Chem. B. 104 (2000) 3481-3487.

(32) M. Kobayashi et al, J. Am. Ceram. Soc. 92 [S1] (2009) S21–S26.

(33) N. Murakami, S. Katayama, M. Nakamura, T. Tsubota, T. Ohno, J. Phys. Chem. C. 115 (2011) 419-424.

(34) T. A. Kandiel, A. Feldhoff, L. Robben, R. Dillert, D. W. Bahnemann, Chem. Mat. 22 (2010) 2050-2060.

(35) M. Kobayashi, K. Tomita, V. Petrykin, S. Yin, T. Sato, M. Yoshimura, M. Kakihana, Solid. State. Phenomena, 124-126, 723-726 (2007)

(36) H. Zhang, J. F. Banfield, J. Phys. Chem. B. 104 (2000) 3481-3487.

(37) M. Kobayashi, V. Petrykin, M. Kakihana, K. Tomita, J. Am. Ceram. Soc. 92 [S1] (2009) S21–S26.

(38) N. Murakami, A. Ono, M. Nakamura, T. Tsubota, T. Ohno, Appl. Catal. B. Environ. 97 (2010) 115–119.

(39) T. Ohno, D. Haga, K. Fujihara, K. Kaizaki, M. Matsumura, J. Phys. Chem. B. 101 (1997) 6415-6419.

(40) N. Murakami, T. Chiyoya, T. Tsubota, T. Ohno, Appl. Catal. A. Gen. 348 (2008) 148.